



Earthworm Cast Formation and Development: A Shift From Plant Litter to Mineral Associated Organic Matter

Alix Vidal^{1,2*}, Françoise Watteau³, Laurent Remusat⁴, Carsten W. Mueller², Thanh-Thuy Nguyen Tu¹, Franz Buegger⁵, Sylvie Derenne¹ and Katell Quenea¹

¹ UMR Milieux Environnementaux, Transferts et Interactions dans les Hydrosystèmes et les Sols (METIS), Sorbonne Université CNRS-EPHE, Paris, France, ² Lehrstuhl für Bodenkunde, TU München, Freising, Germany, ³ INRA, LSE, Université de Lorraine, Nancy, France, ⁴ Muséum National d'Histoire Naturelle, Sorbonne Université, UMR CNRS 7590, IRD, Institut de Minéralogie, de Physique des Matériaux et de Cosmochimie, IMPMC, Paris, France, ⁵ Institute of Biochemical Plant Pathology, Helmholtz Zentrum München, German Research Center for Environmental Health, Neuherberg, Germany

OPEN ACCESS

Edited by:

María Luz Cayuela,
Center for Edaphology and Applied
Biology of Segura (CSIC), Spain

Reviewed by:

Andrey S. Zaitsev,
University of Giessen, Germany
Philippe Cambier,
Institut National de la Recherche
Agronomique (INRA), France

*Correspondence:

Alix Vidal
alix.vidal@wzw.tum.de

Specialty section:

This article was submitted to
Soil Processes,
a section of the journal
Frontiers in Environmental Science

Received: 05 November 2018

Accepted: 05 April 2019

Published: 24 April 2019

Citation:

Vidal A, Watteau F, Remusat L,
Mueller CW, Nguyen Tu T-T,
Buegger F, Derenne S and Quenea K
(2019) Earthworm Cast Formation and
Development: A Shift From Plant Litter
to Mineral Associated Organic Matter.
Front. Environ. Sci. 7:55.
doi: 10.3389/fenvs.2019.00055

Earthworms play a major role in litter decomposition, in processing soil organic matter and driving soil structure formation. Earthworm casts represent hot spots for carbon turnover and formation of biogeochemical interfaces in soils. Due to the complex microscale architecture of casts, understanding the mechanisms of cast formation and development at a process relevant scale, i.e., within microaggregates and at the interface between plant residues, microorganisms and mineral particles, remains challenging. We used stable isotope enrichment to trace the fate of shoot and root litter in intact earthworm cast samples. Surface casts produced by epi-anecic earthworms (*Lumbricus terrestris*) were collected after 8 and 54 weeks of soil incubation in mesocosms, in the presence of ¹³C-labeled Ryegrass shoot or root litter deposited onto the soil surface. To study the alteration in the chemical composition from initial litter to particulate organic matter (POM) and mineral-associated organic matter (MOM) in cast samples, we used solid-state ¹³C Nuclear Magnetic Resonance spectroscopy (¹³C-CPMAS-NMR) and isotopic ratio mass spectrometry (EA-IRMS). We used spectromicroscopic approach to identify plant tissues and microorganisms involved in plant decomposition within casts. A combination of transmission electron microscopy (TEM) and nano-scale secondary ion mass spectrometry (NanoSIMS) was used to obtain the distribution of organic carbon and δ¹³C within intact cast sample structures. We clearly demonstrate a different fate of shoot- and root-derived organic carbon in earthworm casts, with a higher abundance of less degraded root residues recovered as particulate organic matter on the short-term (8 weeks) (73 mg.g⁻¹ in Cast-Root vs. 44 mg.g⁻¹ in Cast-Shoot). At the early stages of litter decomposition, the chemical composition of the initial litter was the main factor controlling the composition and distribution of soil organic matter within casts. At later stages, we can demonstrate a clear reduction of structural and chemical differences in root and shoot-derived organic products. After 1 year, MOM clearly dominated the casts (more than 85% of the total OC in the MOM fraction). We were able to highlight the shift from a system dominated by free plant residues to a system dominated by MOM during cast formation and development.

Keywords: carbon isotopic labeling, root and shoot litter, microorganisms, NanoSIMS, TEM, ¹³C-CPMAS-NMR

INTRODUCTION

Plant residues represent the main contributor to soil organic matter (SOM), followed by microorganism biomass. Among plant residues, the distinction between above (leaves and shoots) and below ground (dead roots and rhizodeposits) inputs is crucial. It is now commonly recognized that roots decompose at a slower rate than shoots and root-derived carbon represents a larger pool of carbon in soils (Balesdent and Balabane, 1996; Puget and Drinkwater, 2001; Lu et al., 2003; Angst et al., 2016). However, whether the slower root decomposition depends on chemical composition, physical or physico-chemical protection, remains unclear, due to the initial location of root in the soil (Rasse et al., 2005).

Biotic factors driving plant residue decomposition encompass the litter quality, as well as the activity of soil fauna and microorganisms (Oades, 1988; Cortez and Bouché, 1998). Soil fauna fragments, transports and partly decomposes residues (Lavelle et al., 1993), and microorganisms decompose and transform organic compounds (Kuzyakov and Blagodatskaya, 2015). Earthworms, ants and termites are considered as the main ecosystem engineers having a significant impact on their environments, under suitable living conditions (Lavelle, 2002; Hastings et al., 2007). In temperate regions, earthworms account for the main invertebrate biomass in soils (Lee, 1985; Edwards, 2004). These saprophagous invertebrates ingest both organic (plant litter, SOM and microorganisms) and mineral soil particles. During ingestion, residues are fragmented and the preexisting soil microstructures destroyed. Organic elements are mixed with mineral particles, complexed with mucus, partly assimilated and mineralized, and mainly released at the soil surface in the form of biogenic organo-mineral aggregates called casts (Lee, 1985; Six et al., 2004). Within a few weeks, the presence of earthworms increases the proportion of macro and microaggregates that are more stable compared with non-biogenic aggregates (Six et al., 2004; Bossuyt et al., 2005; Zangerlé et al., 2011). The mutualistic relationship maintained between earthworms and microorganisms enhance litter decomposition during the gut transit and in casts (Brown et al., 2000). This results in higher microbial activity within casts compared to bulk soil at the scale of days and weeks (Frouz et al., 2011), inducing hotspots of microbial activity (Decaëns, 2010; Kuzyakov and Blagodatskaya, 2015; Athmann et al., 2017). However, casts are among the most complex and dynamic structures in soil (Lee, 1985) and were recognized as potentially favoring long-term carbon protection (Martin, 1991; Bossuyt et al., 2005; Frouz et al., 2009; Sánchez-de León et al., 2014). The occlusion of SOM within microaggregates, which can be found in casts, tends to protect organic carbon (OC) from decomposition (Chenu and Plante, 2006; Lützow et al., 2006; Dignac et al., 2017).

Many relevant processes in earthworm casts happen at a fine spatial scale, i.e., within microaggregates and at the interface between plant residues, microorganisms and mineral particles. As the gut passage leads to a fine scale mixing of mineral and organic soil constituents together with earthworm-derived mucus and bacteria, the resulting casts show a highly complex microscale architecture (Vidal et al., 2016b). To gain

a more fundamental understanding of the processes at the biogeochemical interfaces at the relevant process scale within the casts, the use of spectromicroscopic imaging techniques allowing for high spatial resolution is necessary. The visualization of OM within undisturbed cast microstructures using spectroscopic and microscopic methods can improve our understanding of plant tissue degradation and their association with mineral particles and microorganisms, at these soil biology hot spots. Due to methodological difficulties, this scale of study has often been left out for large scale investigations (Hastings et al., 2007), and studies depicting the role of earthworm casts in the formation and transformation of SOM at the fine scale are scarce (Barois et al., 1993; Pey et al., 2014; Vidal et al., 2016b).

Existing studies focused on revealing cast constituents at a given date, without discerning possible differences with respect to the processing of different substrate materials (Barois et al., 1993; Pey et al., 2014; Vidal et al., 2016b). As main plant-derived SOM constituents, roots and shoots represent a major source for OM during the buildup of cast-rich soils. However, while it is recognized that roots and shoots have contrasted fates in soil, little is known on the ability of earthworms to ingest and transform roots (Curry and Schmidt, 2007; Zangerlé et al., 2011; Cameron et al., 2014), and its impact on root decomposition in casts. The physico-chemical processing of plant residues during the gut passage, coupled to the intense microbial activity and the formation of organo-mineral associations in casts compared with soil, questions the different decomposition processes depicted for roots and shoots in soils. This could significantly influence the carbon cycling and storage in soils, considering that casts might account for at least half of the surface soil layer in natural conditions (Ponomareva, 1950; Lee, 1985).

The present study aimed at highlighting the transfer of plant-derived C and the stage of decomposition of incorporated residues into casts over time. We hypothesized that the chemical characteristics of shoot residues will drive their rapid degradation compared to root residues, and that associations between organic and mineral particles within cast will develop over time. Cast samples, produced in the presence of ^{13}C -labeled shoots and roots, were collected 8 and 54 weeks after the beginning of a mesocosm experiment. The change in the amount and isotopic composition of OM from initial plant residues to particulate organic matter (POM) and mineral-associated OM (MOM) was determined by isotope ratio mass spectrometry (EA-IRMS). Particulate OM and MOM were studied separately to differentiate the free from partly occluded plant residues, respectively. The alteration of the chemical composition of the POM and MOM derived from the casts with time was determined using solid-state ^{13}C cross polarization magic angle spinning nuclear magnetic resonance spectroscopy (^{13}C CPMAS NMR). So as to follow the decomposition processes in intact cast samples at the microscale, we combined elemental and isotopic information obtained with nano-scale secondary ion mass spectrometry (NanoSIMS) with high-resolution information on the arrangement of organic and mineral constituents obtained with transmission electron microscopy (TEM). In previous works, we focused on the method development and technical requirements of the micro-scale analyses (Vidal et al., 2016b) and demonstrated soil alteration due

TABLE 1 | Characteristics of initial soil, as well as Cast-Control, Cast-Root and Cast-Shoot samples over time, before fractionation in POM and MOM (numbers in parentheses indicate the standard deviation, $n = 3$).

| | | Initial soil | Cast-control | | Cast-shoot | | Cast-root | |
|------------------|-------------|--------------|--------------|-------------|------------|-------------|------------|------------|
| | | | 8 weeks | 54 weeks | 8 weeks | 54 weeks | 8 weeks | 54 weeks |
| OC | $mg.g^{-1}$ | 12.1 | 19.0 (2.2) | 16.8 (2.5) | 34.9 (1.2) | 20.6 (1.6) | 55.0 (0.8) | 22.2 (0.6) |
| N content | $mg.g^{-1}$ | 1.30 | 1.97 (0.2) | 1.73 (0.2) | 3.33 (0.1) | 2.03 (0.21) | 3.77 (0.1) | 2.10 (0.1) |
| C/N | | 9 | 10 (0.5) | 10 (0.3) | 11 (0.1) | 10 (0.3) | 15 (0.3) | 11 (0.2) |
| $\delta^{13}C$ | ‰ | -28.1 | -25.3 (1.3) | -28.6 (0.1) | 938 (3.0) | 168 (1.9) | 673 (25) | 127 (8.2) |
| Litter-derived C | % | - | - | - | 58.1 (0.2) | 11.8 (0.1) | 51.8 (1.8) | 11.5 (0.6) |

to earthworm activity using bulk measurements and molecular analyses (Vidal et al., 2016a, 2017). We now use the developed methods and bulk analyses in addition to fractionation and NMR analyses to demonstrate the fine scale mechanisms of litter degradation through time. This approach reflects the increasing cognition in environmental science for the need to combine imaging with classical bulk measurements to gain a deeper understanding of biogeochemical processes (Mueller et al., 2013; Baveye et al., 2018).

MATERIALS AND METHODS

Experimental Setup

Three mesocosms were filled with ~75 L of a loamy-sand soil (clay, 19%; silt, 25%; sand, 56%) collected on permanent grassland in North of France (Oise, France). The soil characteristics are described in **Table 1** and available in Vidal et al. (2017) and Vidal (2016). Mesocosms were placed in a greenhouse where soil humidity and temperature were maintained at 23% and 13°C, respectively. Six *Lumbricus terrestris* earthworms were deposited onto each mesocosm.

Plants of Italian Ryegrass (*Lolium multiflorum*) were artificially labeled in ^{13}C at the PHYTOTEC platform of the Alternative Energies and Atomic Energy Commission (CEA) in Cadarache (France). Plants were grown under a controlled and constant $^{13}CO_2$ enriched atmosphere (2.6% $^{13}CO_2$). The mean $\delta^{13}C$ values were 1,632 ‰ (± 16) and 1,324 ‰ (± 42) for shoots and roots, respectively. Shoots and roots were separated, dried and subsequently homogenized separately during 40 s with a laboratory blender (Waring Commercial) in order to obtain small fragments with millimeter size. We deposited 250 g of shoots and roots (~0.9 g OC.kg soil $^{-1}$) on the soil surface of the two mesocosms, respectively. Although the design does not reflect the real condition of *in situ* root systems, both roots and shoots were voluntarily deposited onto the soil surface, under the same conditions, in order to consider the sole effect of the chemical composition of litter (without any initial physical contact of the roots with the soil particles) on its incorporation and decomposition in earthworm casts. No litter was applied on the third mesocosm, which served as control. After 8 and 54 weeks of experiment, around 10 earthworm cast fragments were randomly collected on the soil surface of each mesocosm using a spatula and combined to form a composite sample of around 50 grams for each time step. The present work aimed at improving

the understanding of fundamental processes by combining bulk chemical and imaging techniques, which together provide a more complete view on small scale soil functioning. As we combined all used techniques on one sample per treatment each, no replication could be achieved due to time concern. The time points of sampling were selected according to the contrasted isotopic and molecular composition measured on bulk samples in previous works (Vidal et al., 2016a, 2017). For example, the shift from more than 50–12% of litter-derived carbon in casts from 8 to 54 weeks (**Table 1**) showed a clear differentiation into a first and second decomposition phase which led to the two chosen sampling dates. Casts were distinguished from the bulk soil due to their round shape and smooth texture (Velasquez et al., 2007). After 8 weeks of experiment most casts were fresh when collected, while after 54 weeks, casts started to age and dry. A sub-sample of 5 grams, made of around three cast fragments, was directly processed for TEM and NanoSIMS analyses after sampling. The rest of the sample was dried, ground and subsequently fractionated into POM and MOM physical soil fractions. The obtained SOM fractions were analyzed for OC, N and $\delta^{13}C$. The chemical composition of the SOM fractions was analyzed using ^{13}C CPMAS NMR spectroscopy. For the cast collected in the mesocosms containing roots, shoots and no litter, we will refer to Cast-Root, Cast-Shoot and Cast-Control, respectively.

Separation of POM and MOM Fractions

In order to differentiate between plant residue dominated and mineral-associated OM, dry and ground cast samples were fractionated to separate POM and MOM. Briefly, 4 g of cast sample were saturated with 50 mL sodium polytungstate solution with a density of 1.8 (TC Tungsten compounds, Grub am Forst, Germany). After settling overnight, the floating free POM was collected using a vacuum pump, washed to remove excess Sodium Polytungstate (conductivity < 3 μS) using pressure filtration (22 μm filter) and freeze-dried. The mineral fraction containing the MOM was washed to remove salts (conductivity < 50 μS), centrifuged (3,000 g, 30 min) and freeze-dried. The density fractionation resulted in a mean recovery of $94 \pm 2.9\%$ of the initial sample mass. In the present study, the POM fraction is considered as the particulate plant residues, which are extractable by floatation in a dense liquid, while the MOM fraction comprises the organo-mineral associations.

Bulk Elemental and Isotopic Analyses

All POM and MOM fractions were analyzed (Helmholtz Zentrum, Munich, Germany) for organic carbon, nitrogen and $\delta^{13}\text{C}$ using IRMS (δV Advantage, Thermo Fisher, Dreieich, Germany) coupled to an Elemental Analyzer (Euro EA, Eurovector, Milan, Italy). An acetanilide standard, calibrated against several suitable international isotope standards (IAEA; Vienna), was used for calibrating. Prior to organic carbon and $\delta^{13}\text{C}$ analyses, MOM fraction samples were decarbonated adding 20 μl of HCl 2N to 1–5 mg samples for 10 h and drying overnight at 60°C. Additional samples were prepared (10–40 mg) for nitrogen analyses.

The labeled litter-derived carbon in POM and MOM fractions of earthworm casts was expressed according to equation 1:

$$\text{Litter-derived C(\%)} = [(\delta^{13}\text{C}_{\text{sample}} - \delta^{13}\text{C}_{\text{control}}) / (\delta^{13}\text{C}_{\text{litter}} - \delta^{13}\text{C}_{\text{control}})] \times 100 \quad (1)$$

Where $\delta^{13}\text{C}_{\text{sample}}$ is the $\delta^{13}\text{C}$ value of the POM or MOM fraction samples isolated from casts incubated with labeled roots or shoots, $\delta^{13}\text{C}_{\text{control}}$ is the $\delta^{13}\text{C}$ value of the POM or MOM fraction samples isolated from control casts incubated without litter, $\delta^{13}\text{C}_{\text{litter}}$ is the $\delta^{13}\text{C}$ values of the labeled roots or shoots.

The percentage OC of the MOM or the POM fraction compared to the total OC contained in both POM and MOM isolated fractions (% OC bulk) was also calculated.

Nuclear Magnetic Resonance Spectroscopy

The ^{13}C -CPMAS-NMR analyses were performed (Chair of Soil Science, TUM, Freising, Germany) on initial litter, as well as POM and MOM fractions of cast samples, using a Bruker AvanceIII 200 spectrometer (Bruker BioSpin GmbH, Karlsruhe, Germany). The NMR was operated at a ^{13}C -resonance frequency of 50 MHz, with a spinning speed of 6.8 kHz and according to the carbon content, a recycle delay time of 2 or 0.4 s, for initial litter and other samples, respectively. From around 1,000 to up to 200,000 scans were accumulated for initial litter and other samples, respectively. The spectra were processed with a line broadening from 0 to 50 Hz, followed by phase adjustment and base line correction. The chemical shift regions were obtained by dividing the NMR spectra as followed: 0–45 ppm (alkyl-C), 45–110 ppm (O-N-alkyl-C), 110–160 ppm (aromatic-C) and 160–220 ppm (carboxyl-C) (Kögel-Knabner et al., 1992). It has to be noted that the 160–220 ppm chemical region also include carbonyl-C, but that the carboxyl-C are by far dominant. The ratio between alkyl-C and O-N-alkyl-C was used as an indicator of organic matter degradation. A higher alkyl-C/O-N-alkyl-C ratio generally reflects a higher OM degradation, as alkyl carbon chains tend to be less degradable compared with carbohydrates and proteins (source of O-N-alkyl-C) (Baldock et al., 1997). Although these values cannot be considered as absolute ones (due to overlapping signals and potential differences in relaxation times between the different types of C), they can be used for comparison purposes.

Ultrastructural Analyses by TEM

The materials and methods used to prepare undisturbed samples for TEM and NanoSIMS analyses were identical to those described in Vidal et al. (2016b). In brief, osmium tetroxide was used to chemically fix cast samples (2 g for each sample) and initial litter parts. To avoid sample disruption, cast structures were physically preserved with agar (Watteau et al., 2006). Cast samples were cut into cubes of few mm^3 (around 10 for each sample), dehydrated in graded acetone series, and embedded in epoxy resin (Epon 812). Ultrathin sections (80–100 nm) were sliced using a Leica Ultracut S ultramicrotome, stained with uranyl acetate and lead citrate and analyzed with a JEOL EMXII transmission electron microscope operating at 80 kV (LSE, Nancy, France).

Nano-Scale Isotope Analyses by NanoSIMS

Ultrathin twin sections of 100–200 nm were sliced from the same blocks prepared for TEM analyses, allowing the comparison between NanoSIMS and TEM images. Samples were gold coated and images were acquired using the NanoSIMS 50 (Cameca, France) located at Museum national d'Histoire naturelle in Paris, France. The sample surface was sputtered by a 1.5 pA Cs^+ beam to obtain $24 \times 24 \mu\text{m}$ images (256×256 pixels) of $^{12}\text{C}^-$, $^{12}\text{C}^{14}\text{N}^-$, $^{13}\text{C}^{14}\text{N}^-$, and $^{28}\text{Si}^-$ secondary ions. The images were processed using the LIMAGE[®] software (L. Nittler, Carnegie Institution, USA). Secondary ion images of $^{12}\text{C}^{14}\text{N}^-$ and $^{28}\text{Si}^-$ were used to distinguish organic structures from mineral particles. The ^{13}C isotopic images, named as $\delta^{13}\text{C}$ in the following, were generated using the $^{13}\text{C}^{14}\text{N}^- / ^{12}\text{C}^{14}\text{N}^-$ ratio relative to the PDB standard. The heterogeneity of the $\delta^{13}\text{C}$ values observed on similar organic structures on NanoSIMS images can either reflect a methodological bias (variable contribution of C from epoxy resin) or a natural process (variable extent of C recycling), both leading to variable degree of isotopic dilution. Given these approximations, $\delta^{13}\text{C}$ values obtained in the present study were considered as indicators of the occurrence of labeled OC, and not taken as representative of accurate isotopic enrichment values.

Statistical Analyses

A principal component analysis (PCA) was performed with the R statistical software (package “FactoMinerR”) on the 12 fraction samples (POM and MOM) using the 4 NMR chemical shift regions as variables. Root and shoot litter samples were implemented as illustrated samples in the PCA. The variables were normally distributed, as tested by the Shapiro-Wilk test.

RESULTS

C and N Elemental and Isotopic Composition, and Distribution in POM and MOM Fractions

At 8 weeks, the mass proportion of POM fraction was higher in Cast-Root compared to Cast-Shoot (73 vs. 44 $\text{mg}\cdot\text{g}^{-1}$, respectively) (Table 2). Particulate OM and MOM (Cast-Shoot

TABLE 2 | Organic carbon, nitrogen, $\delta^{13}\text{C}$ and chemical characteristics of particulate organic matter (POM) and mineral associated organic matter (MOM) fractions isolated from earthworm casts.

| | | | Cast-control | | Cast-shoot | | Cast-root | |
|-----|-----------------------------|--------------------|--------------|----------|------------|----------|-----------|----------|
| | | | 8 weeks | 54 weeks | 8 weeks | 54 weeks | 8 weeks | 54 weeks |
| POM | Mass proportion of fraction | mg.g^{-1} | 14 | 11 | 44 | 15 | 73 | 8 |
| | OC | mg.g^{-1} | 95 | 105 | 306 | 171 | 317 | 139 |
| | Total OC | mg | 5 | 5 | 54 | 10 | 93 | 5 |
| | %C of bulk | | 9 | 11 | 42 | 15 | 43 | 7 |
| | N content | mg.g^{-1} | 7 | 7 | 21 | 12 | 14 | 9 |
| | C/N | | 15 | 15 | 14 | 14 | 23 | 16 |
| | $\delta^{13}\text{C}$ | ‰ | -28 | -28 | 1,177 | 87 | 935 | 185 |
| | Litter-derived C | % | - | - | 73 | 7 | 71 | 16 |
| | Alkyl-C/O-N-alkyl-C | | 0.43 | 0.40 | 0.25 | 0.46 | 0.11 | 0.35 |
| MOM | Mass proportion of fraction | mg.g^{-1} | 952 | 900 | 917 | 955 | 879 | 886 |
| | OC | mg.g^{-1} | 15 | 11 | 21 | 15 | 35 | 17 |
| | Total OC | mg | 57 | 39 | 76 | 58 | 124 | 60 |
| | %C of bulk | | 91 | 89 | 58 | 85 | 57 | 93 |
| | N content | mg.g^{-1} | 1 | 1 | 2 | 1 | 2 | 1 |
| | C/N | | 12 | 13 | 12 | 11 | 15 | 13 |
| | $\delta^{13}\text{C}$ | ‰ | -28 | -28 | 754 | 198 | 846 | 190 |
| | Litter-derived C | % | - | - | 47 | 14 | 65 | 16 |
| | Alkyl-C/O-N-alkyl-C | | 0.42 | 0.50 | 0.38 | 0.49 | 0.17 | 0.38 |

The total organic carbon (Total OC) values were calculated using POM or MOM fraction masses. The % OC of bulk corresponds to the percentage of OC in POM or MOM fractions compared to the sum of the OC in POM and MOM fractions.

and Cast-Root) fractions contained around 40 and 60% of the total OC isolated, respectively (Table 2). Cast-Control POM and MOM fractions contained around 10 and 90% of the OC of bulk casts, respectively. In both Cast-Shoot and Cast-Root fraction samples, at least 50% of OC was litter-derived, with a higher percentage in Cast-Root MOM fraction (65%) compared to Cast-Shoot MOM fraction (47%). At 54 weeks, the mass proportion of MOM fraction slightly increased compared with 8 weeks and more than 85% of the total OC isolated was contained in the MOM fractions of both Cast-Shoot and Cast-Root. In both POM and MOM fractions, the litter-derived carbon dropped to 15%, with a minimum of 7% in the Cast-Shoot POM fraction. The C/N ratio decreased, compared with 8 weeks, of 30% and 13% in the Cast-Root POM and MOM fractions, respectively.

Chemical Characterization of Cast POM and MOM Fractions

Initial roots and shoots presented similar NMR spectra clearly dominated by carbohydrates (O-N-alkyl-C) (Figure 1). In initial roots, the relative abundance of alkyl-C was lower, while the relative abundance of aromatic-C was slightly higher than shoots (Figures 1B,C and Table S1). At 8 weeks, spectra for the POM fraction of Cast-Root and Cast-Shoot presented similar characteristics as the initial litter (Figures 1B,C), while those of MOM fraction spectra were broader (Figures 1E,F). At 54 weeks, a general broadening of spectra was observed for both POM and MOM fractions (Figure 1). A PCA was carried out to highlight the chemical characteristics of organic matter in POM and MOM isolated from earthworm casts after 8 and 54 weeks

of experiment (Figure 2). The two factors (F1, F2) generated by the PCA explained 97% of the variance. F1 clearly separated Cast-Control samples and 54-week samples from Cast-Shoot and Cast-Root samples collected at 8 weeks (Figure 2B). Cast-Control samples were represented by a high relative abundance of aromatic-C and carboxyl-C, while 8 week Cast-Shoot and Cast-Root samples contained higher relative abundance of O-N-alkyl-C. At 8 weeks, the Cast-Root MOM fraction remained relatively close to the Cast-Root POM fraction and the initial root chemical characteristics. In contrast, Cast-Shoot MOM fraction at 8 weeks presented similar characteristics to the samples collected after 54 weeks. After 54 weeks, the OM in Cast-Shoot and Cast-Root samples tended to evolve toward Cast-Control chemical characteristics (Figure 2). Compared with 8 weeks, the relative abundance of O-N-alkyl-C decreased, while that of alkyl-C and aromatic-C increased (Figure 2B), resulting in a higher alkyl-C/O-N-alkyl-C ratio for both Cast-Root and Cast-Shoot (Table 2).

Cast-Root and Cast-Shoot at the Microscale

Structures of intact cast samples were analyzed with TEM and NanoSIMS in order to obtain detailed information of the microscale spatial assembly of the biogeochemical interfaces. At 8 weeks, plant residues incorporated in earthworm casts presented similar structures compared to the initial shoots and roots (Figures S1, S2), although they showed different degradation stages (Figure 3). For example, parenchyma cells were partially degraded in Cast-Shoot

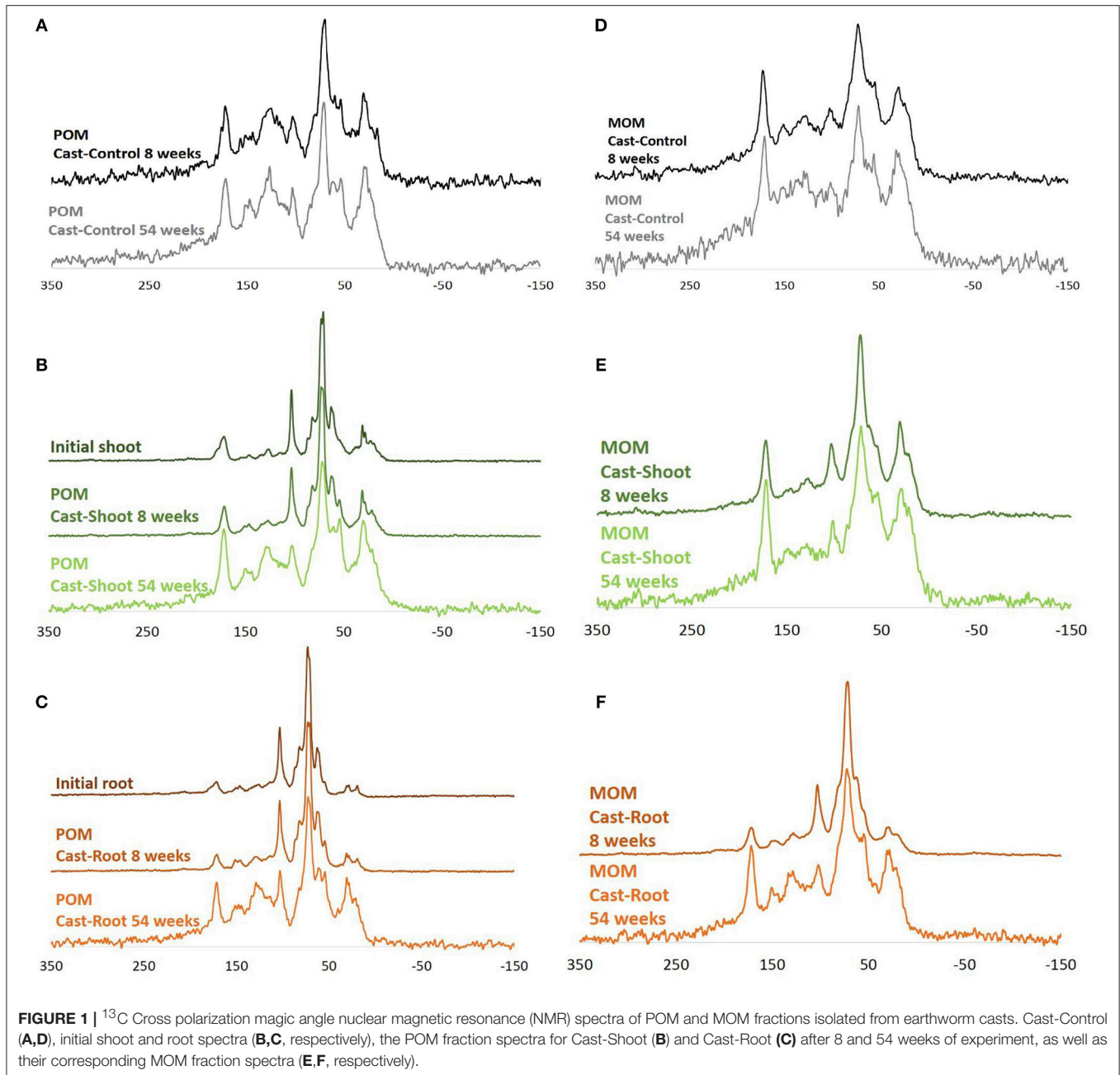
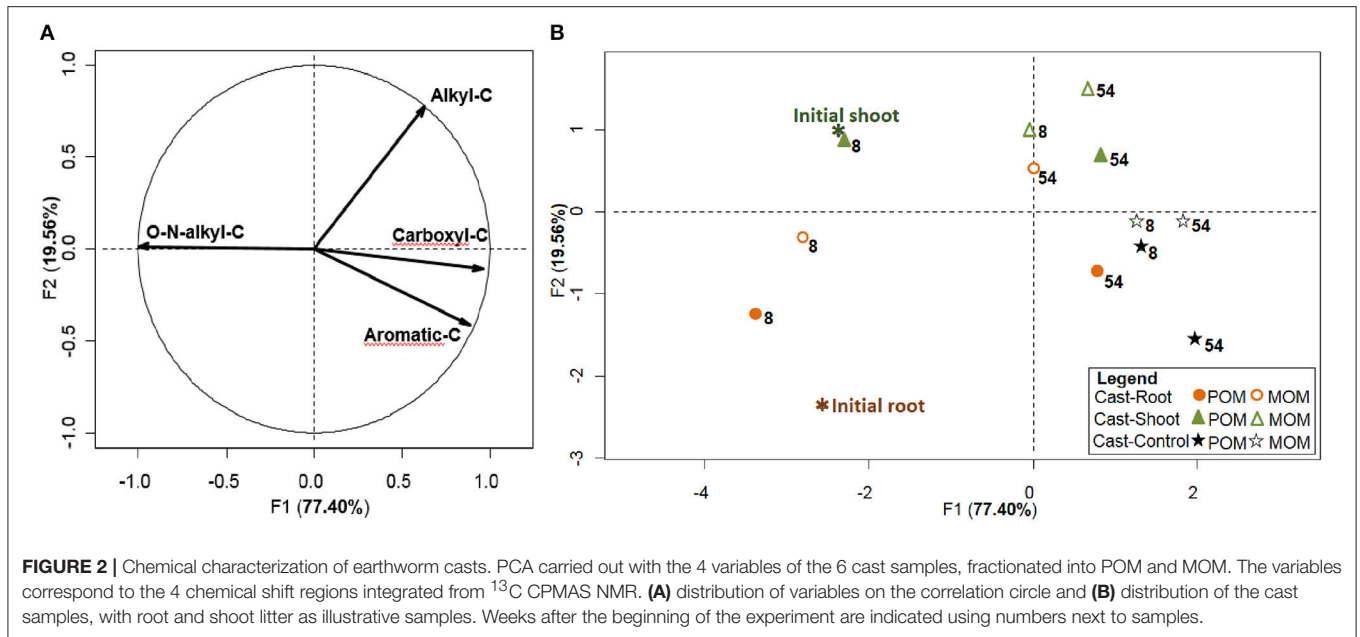


(**Figure 3A**) compared with initial shoot tissues (**Figure S1A**), while woody tissues were well preserved (**Figure 3A**). Both Cast-Shoot and Cast-Root images highlighted some preserved plant tissues (**Figures 3A,G**), long and thin laces identified as parenchyma cell wall residues (**Figures 3B,F,H**), microaggregates (**Figures 3B,I, 4A,B**) and microorganisms (**Figures 3C–E,H**). Intact or barely degraded plant structures were prevalent in Cast-Root (**Figures 3G,H**). Various microorganisms, mainly fungi and bacteria, were depicted within Cast-Shoot: fungi attacking cell walls of woody tissues (**Figure 3D**), bacteria colonizing parenchyma cells (**Figure 3E**), or microorganisms within microaggregates (**Figure 3C**).

A few microorganisms were also observed in Cast-Root (**Figures 3G,H**).

Many features identified in TEM images were recognized in NanoSIMS images. For Cast-Shoot, **Figures 4A,B** were comparable to **Figures 3C,B**, respectively, with the clear occurrence of a labeled fungus (**Figure 4A**), amorphous OM and plant cell wall (**Figure 4B**). On these images, $^{28}\text{Si}^-$ maps reflect an important proportion of small size mineral particles (i.e., mainly clay size $< 2\ \mu\text{m}$) on images and $^{12}\text{C}^{14}\text{N}^-$ maps showed organic structures among these mineral particles. Cast-Shoot images showed the presence of partially degraded plant structures derived from the labeled plants and labeled



microorganisms involved in plant decomposition (Figures 4A,B, respectively). Degraded plant structures and microorganisms were both integrated into organo-mineral aggregates. For Cast-Root, Figures 4C,D were comparable to Figures 3G,H. Labeled plant structures observed on NanoSIMS Cast-Root images presented a lower degree of degradation and reduced associations with mineral particles (Figures 4C,D), compared with Cast-Shoot images.

At 54 weeks, microaggregates (from 20 to 30 μm) with complex organo-mineral composition, were frequently observed on Cast-Shoot (Figures 5A–C) and Cast-Root (Figure 5G) images. Highly degraded plant tissues, cell walls or amorphous organic residues were prevalent in Cast-Shoot. Residues of woody tissues were still recognizable and colonized by bacteria (Figure 5D). On Cast-Root images, some cell wall residues surrounded by mineral particles were identified (Figure 5E) and some cell intersections were still recognizable (Figure 5F). Microorganisms were prevalent on both Cast-Shoot and Cast-Root images. Bacteria were either intact, present under residual form (dead microorganisms leaving cell wall residues) (Figures 5B,D; Figures 5E,H) or spores (presenting dark core and coat) (Figures 5B,H).

On NanoSIMS images, labeled areas were scarce (Figure 6) compared with samples observed after 8 weeks of experiment (Figure 4). Three types of labeled structures are identified on Cast-Shoot and Cast-Root images: (1) well-defined spots corresponding to bacteria (Figure 6C) or fungi (Figure 6D), (2) organic structures similar to cell wall residues (Figure 6B) and (3) “diffused” labeling probably corresponding to highly degraded organic structures (Figure 6A). $\delta^{13}\text{C}$ values are highly variable on all images, with $165\text{‰} < \delta^{13}\text{C} < 1131\text{‰}$ in structures identified as microorganisms on Cast-Root (7 images observed, data not shown). No clear differences in $\delta^{13}\text{C}$ values were observed between Cast-Root and Cast-Shoot.

DISCUSSION

Litter Type has a Short-Term Impact on Cast Composition Which Is Smoothed on the Longer Term

As mentioned above, root and shoot materials were both deposited onto the soil surface in the same conditions to focus on the impact of the sole chemical composition of litter type, without considering physical interactions between roots and soil. Even though other soil biota and physico-chemical processes may play a role in litter degradation, the action of earthworms is major in temperate soils. The present study focuses on this action through the analysis of root and shoot incorporation within casts. Although it is difficult to generalize the obtained results to soils, it must be noted that casts might account for half of the soil surface layer in natural systems containing earthworms (Ponomareva, 1950; Six et al., 2004).

At 8 weeks, the high percentage of litter-derived carbon in Cast-Root and Cast-Shoot (Table 2), their proximity in chemical composition with the corresponding initial plant residues revealed by the PCA (Figure 2), as well as the observation of plant structures within casts (Figures 3, 4), highlighted the capacity of earthworms to incorporate both shoots and roots in casts. However, some differences could be evidenced between Cast-Root and Cast-Shoot at 8 weeks, which reflect different incorporation and/or decomposition extents for the two types of plant residues. Indeed, Cast-Root can be distinguished from Cast-Shoot by a higher quantity of plant residues isolated as POM, a higher labeling and C/N ratio (Table 2) a lower level of degradation of the observed plant structures (Figures 3, 4), as well as a higher relative abundance of O-N-alkyl-C (Figure 2), as typically observed for fresh residues (Lorenz et al., 2007). These results suggested either a delayed incorporation of roots

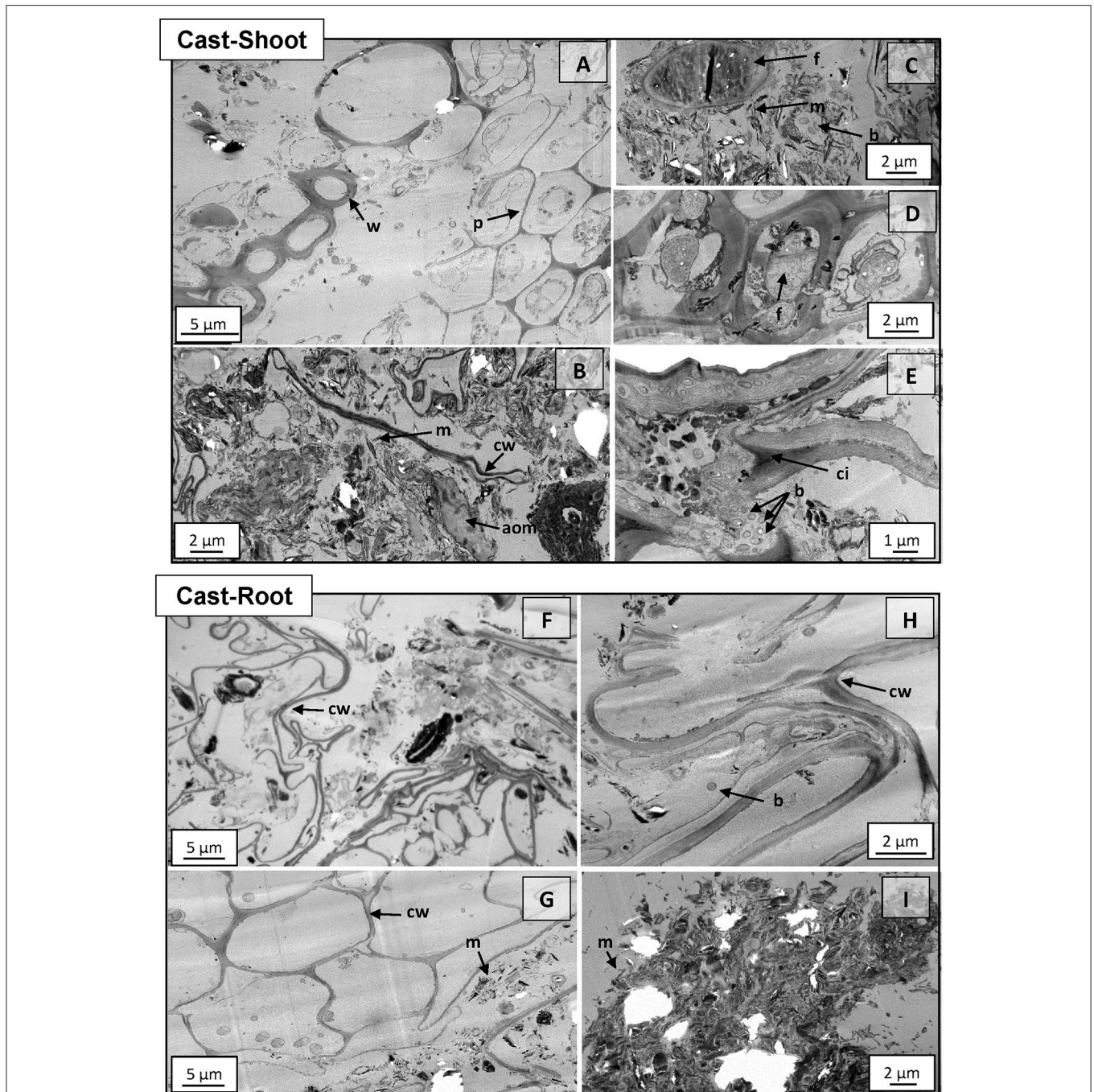


FIGURE 3 | TEM micrographs of Cast-Shoot and Cast-Root samples after 8 weeks of experiment. **(A)** Partially degraded parenchyma cells and well-preserved woody tissues; **(B)** organo-mineral aggregate; **(C)** fungus in an organo-mineral aggregate; **(D)** fungi attacking woody tissues; **(E)** bacteria inside cell walls; **(F,H)** compacted cell walls; **(G)** intact cell walls and **(I)** organo-mineral aggregate dominated by mineral particles. aom, amorphous organic matter; b, bacteria; cw, cell wall; ci, cell intersection; f, fungus; m, mineral particle; p, parenchyma cell; w, woody tissue.

by earthworms and/or a slower decomposition of roots in casts. Both hypotheses are plausible, as the root lignin content (aromatic-C relative abundance, **Table S1**) makes roots less palatable for earthworms (delayed incorporation) (Tian et al., 1995) and slower to decompose (Balesdent and Balabane, 1996; Puget and Drinkwater, 2001; Lu et al., 2003). The difference in

plant decomposition is also corroborated by the clear difference in the C/N ratio of the initial roots compared with shoots (30.7 vs. 14.8) (Vidal et al., 2017). We were thus able to demonstrate a clear relationship between the chemical composition of the type of applied plant residue and its short-term degradation as promoted by earthworm and microorganism activity.

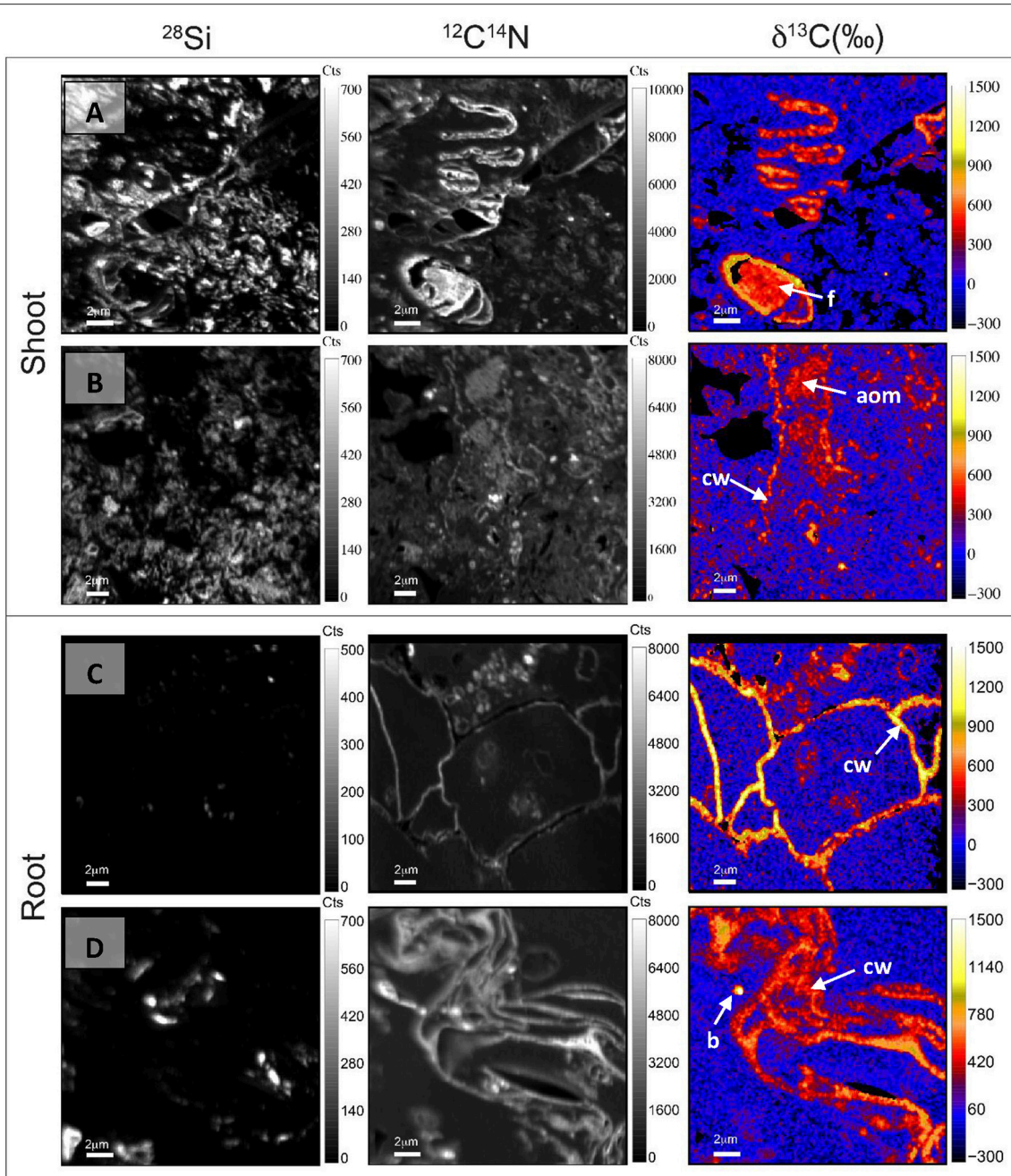
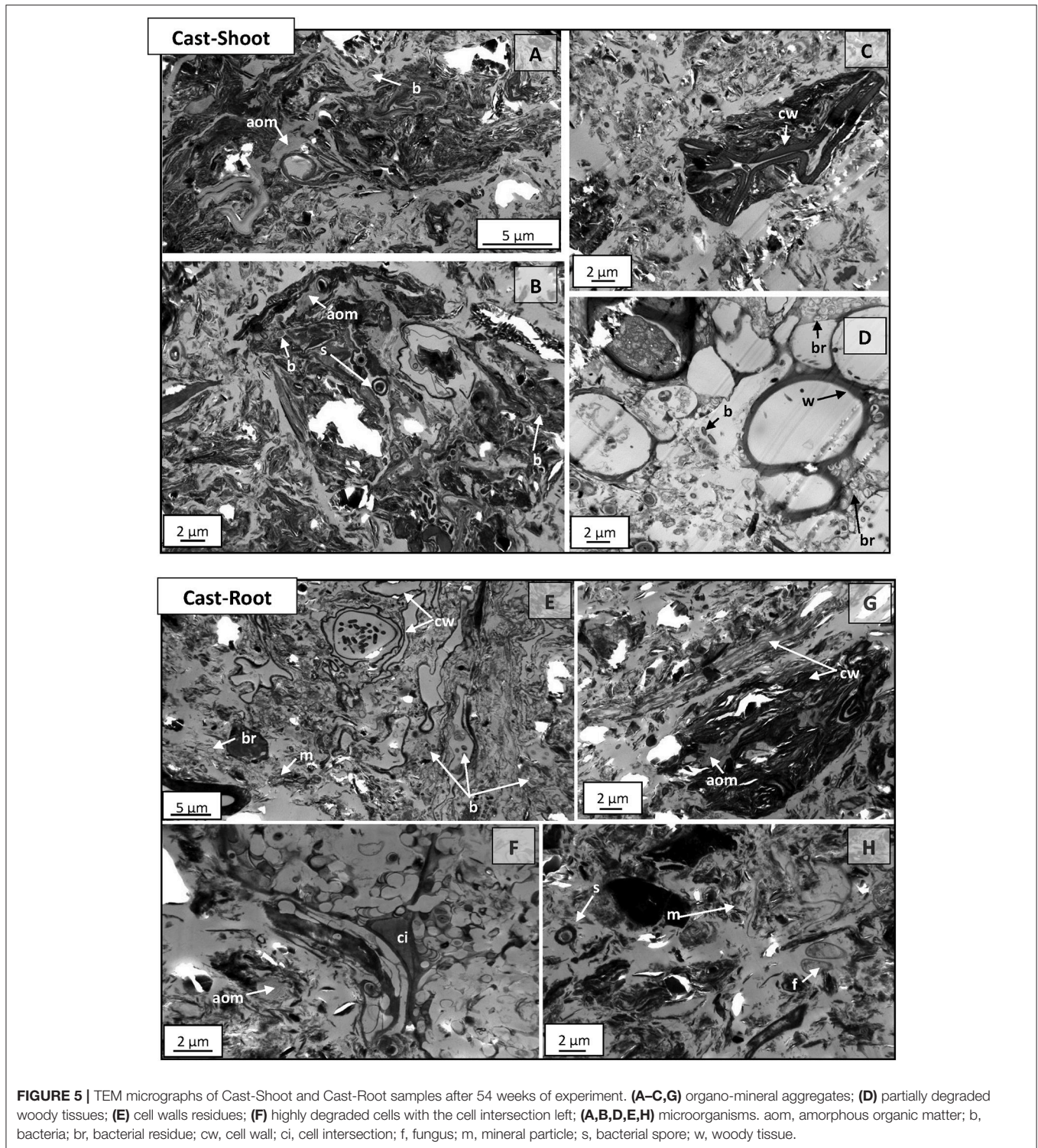


FIGURE 4 | NanoSIMS maps of $^{28}\text{Si}^-$, $^{12}\text{C}^{14}\text{N}^-$, and $\delta^{13}\text{C}$ illustrating contrasted degradation stages of labeled plant tissues and microorganisms implied in their decomposition, after 8 weeks of experiment, for both Cast-Shoot (**A,B**) and Cast-Root (**C,D**). aom, amorphous organic matter; b, bacteria; cw, cell wall; f, fungus.

Studies depicting the impact of earthworms on soil carbon cycle are mainly restricted to short-term experiments (<200 days) (Lubbers et al., 2013). The present study tracked litter-derived C for more than 1 year in earthworm casts. The aforementioned structural and chemical differences between Cast-Root and Cast-Shoot were reduced after 54 weeks, highlighting the capacity of earthworms to efficiently degrade both shoots and roots. The chemical changes in casts between 8

and 54 weeks reflected a commonly illustrated litter decay process (Baldock and Skjemstad, 2000; Lorenz et al., 2007; Mueller et al., 2009, 2014; Preston et al., 2009; Cepáková and Frouz, 2015). The decrease in POM quantity and plant-derived-C (**Table 2**) highlighted the degradation of plant residues, via the loss of labile carbon and mineralization (Cotrufo et al., 2015). This was corroborated by the alkyl-C/O-N-alkyl-C ratio increase in POM and MOM fractions (**Table 2**) which reflected a relative decrease



in easily degradable compounds such as carbohydrates (O-N-alkyl-C) and/or a relative accumulation of biologically stable polymethylenic compounds (alkyl-C) including hydrophobic by-products of decomposition (Bonanomi et al., 2013). The relative increase in aromatic-C (**Figure 2** and **Table S2**) indicated

a higher contribution of lignin-derived compounds in plant residues (Angst et al., 2016). These chemical changes were correlated to microscopic observations, as remaining plant structures were represented by structural plant parts (e.g., cell walls, cell intersections and woody tissues) (**Figure 5**) which

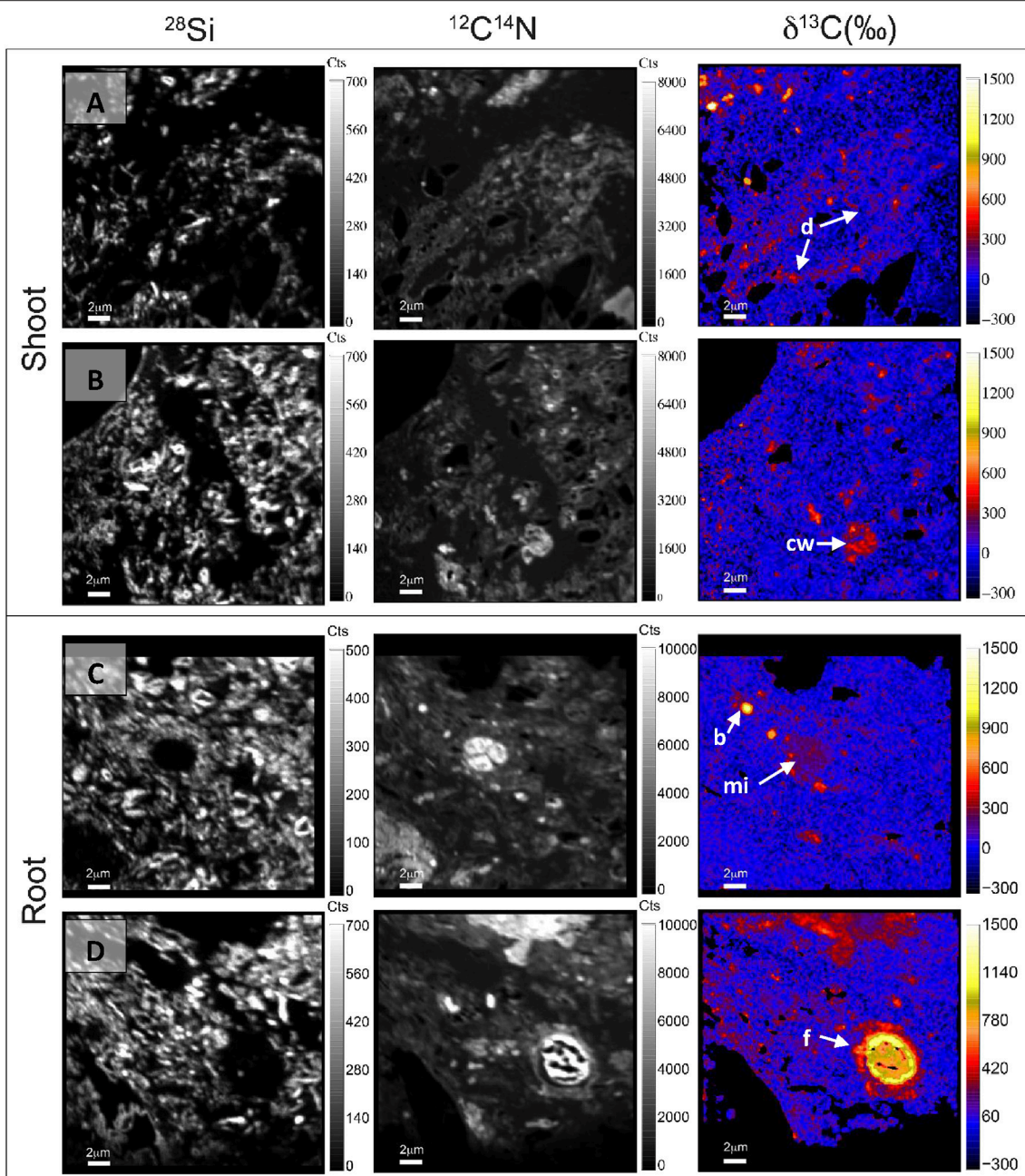


FIGURE 6 | NanoSIMS maps of $^{28}\text{Si}^-$, $^{12}\text{C}^{14}\text{N}^-$, and $\delta^{13}\text{C}$ illustrating the integration of labeled organic structures (both plant tissues and microorganisms) inside organo-mineral aggregates, after 54 weeks of experiment, for both Cast-Shoot (**A,B**) and Cast-Root (**C,D**). b, bacteria; cw, cell wall; d, “diffused” labeling; f, fungus; mi, microorganism (bacteria or fungi).

show higher resistance to degradation and generally present higher lignin concentrations compared to non-structural parts (Fahey et al., 2011; Jouanin and Lapierre, 2012; Cotrufo et al., 2015). The bacteria or bacterial residues associated to woody tissues (**Figure 5D**) were also a sign for advanced degradation.

These results are consistent with recent findings highlighting that although earthworms avoid phenolic-rich

substrates, such as roots, they tend to accelerate their degradation with time (Bi et al., 2016; Angst et al., 2017). The short-term impact of the litter type was smoothed at the longer term, which strengthened the need to consider the long-term (> 200 days) role of earthworms on litter decomposition and carbon cycling (Lubbers et al., 2013; Angst et al., 2017).

Connecting Litter Decomposition Features With Microorganisms

Thanks to NMR spectroscopy and EA-IRMS analyses on fractionated cast material, we were able to depict the plant degradation stages and the contribution of mineral-associated organic matter along the year of experiment. In intact samples, i.e., considering the complex microscale architecture of casts, TEM and NanoSIMS revealed information on the location and structural evolution of plant residues along degradation, as well as on the microorganisms feeding on these residues.

The lower amount of intact shoot structures (vs. root) in casts at 8 weeks (**Figures 3, 4**) can be related to the abundance and diversity of the observed microorganisms. Indeed, a clear contribution of specific microorganisms to shoot degradation is evidenced by their colonization of partly degraded shoot structures (**Figures 3D,E**) associated with their high isotopic enrichment (**Figure 4A**). Abundant microbial communities have frequently been observed in fresh earthworm casts due to the high amount of available substrate (i.e., mucus, plant structures) (Parle, 1963; Drake and Horn, 2007; Frouz et al., 2011), partly released during the digestion activities of the earthworms (Brown et al., 2000). These microorganisms tend to use the more labile and easily available content first (e.g., cell contents) (Fahey et al., 2011), the latter representing their main source of energy and carbon (Cotrufo et al., 2015). This was reflected by the extensive biodegradation of parenchyma cells, while woody tissues often remained intact (**Figure 3A**) and corroborated by the slight relative increase in lignin-derived signals in the NMR spectra of the POM fractions (vs. initial shoots) (**Tables S1, S2**). Moreover, the diversity of microorganism metabolic capacities in casts (Brown, 1995) is illustrated by the occurrence of some bacterial clusters associated to plant cell walls (**Figure 3E**) and of fungi, attacking cell walls (**Figure 3D**). As earthworms are not able to decompose lignin without the participation of microorganisms (Neuhauser et al., 1978; Curry and Schmidt, 2007), the degradation of woody tissues was initiated by fungi, which are able to degrade more resistant tissues compared to bacteria (Bossuyt et al., 2001) and are particularly implied in lignin decomposition (Tuor et al., 1995; Filley et al., 2002; Dignac et al., 2005). The action of fungi provided bacteria with intermediate decomposition products and enable their colonization of woody tissues (Roman et al., 2006).

While most microorganism cells identified at 8 weeks were in an intact form, they exhibited various stages of structural degradation at 54 weeks (**Figures 5, 6**). In parallel, the OC content decreased in casts (**Table 1**), the substrates started to become less decomposable (e.g., increase in lignin-derived compounds), entrapped within microaggregates (**Table 2** and **Figure 2**) and thus limiting for microorganisms, which could progressively starve (Miltner et al., 2012). Indeed, organo-mineral interactions have been previously reported as one of the main drivers for SOM stabilization, leading to a restriction in substrate bioavailability and diffusion (Mueller et al.,

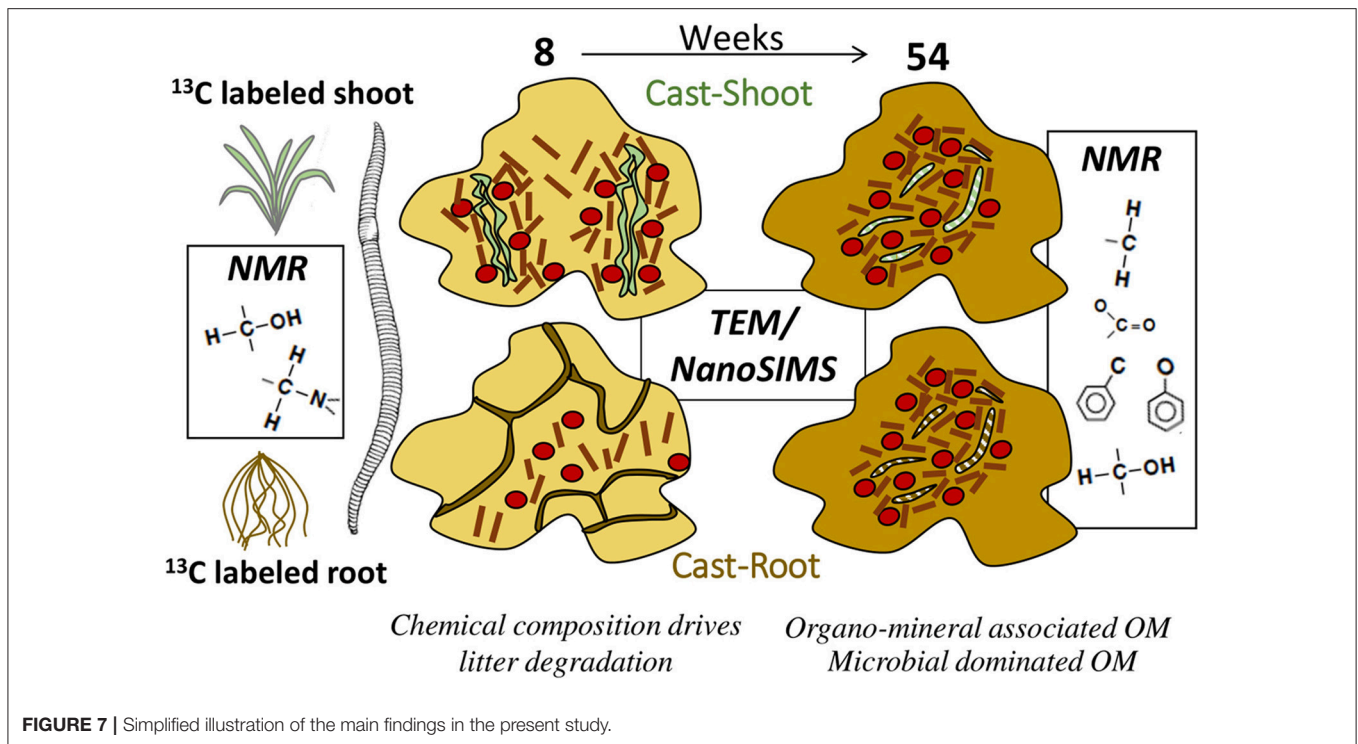
2014; Angst G. et al., 2017). With a decrease in substrate bioavailability some bacteria formed spores (**Figures 5B,H**). The sporulation might either be caused by the anoxic conditions created during the earthworm gut transit or by the lack of substrate (Brown, 1995; Drake and Horn, 2007). The exhaustion of easily available substrate can also lead to the starvation of microorganisms and the autolysis of bacterial cells (van Veen et al., 1997; Zelenev et al., 2000; Ekschmitt et al., 2005). Thus, other bacteria which were not able to overcome this lack of energy and carbon died and were left as bacterial residues (**Figures 5B–E**) (Miltner et al., 2012).

Thus, with the decay of the litter-derived OM, we could show the parallel buildup of microbial dominated OM. This is also supported by the decrease in C/N ratios in Cast-Root POM and MOM fractions (**Table 2**) that reflect the decay of litter and the relatively higher microbial contribution (Mueller et al., 2014; Cepáková and Frouz, 2015). The presence of labeled microorganisms enclosed within microaggregates (**Figures 6C,D**) pointed to the limitation of the accessibility of microbial-derived OC for degradation. The spatial inaccessibility created by this process could lead to a protection of this microbial-derived OC from degradation (Lützwow et al., 2006; Shan et al., 2013) and could represent a source of carbon at the longer term (Miltner et al., 2012).

Organo-Mineral Associations Prevailed After 1 Year

At 54 weeks, there was a relative shift from a POM-dominated to a MOM-dominated system. Organo-mineral associations prevailed in casts, as supported by the high percentage of OC of bulk in MOM fractions (**Table 2**) and the abundance of microaggregates with high mineral contribution on TEM and NanoSIMS images (**Figures 5, 6**). Thus, after the destruction of existing microstructure during the gut transit (Shipitalo and Protz, 1989; Six et al., 2004), new microaggregates developed in casts under the combined effect of mineral properties (e.g., adsorption capacities) and microorganism activity. Interactions between minerals and OM are partly controlled by mineral features, such as mineralogy and chemical compositions influencing their capacity to adsorb organic material (Baldock and Skjemstad, 2000; Eusterhues et al., 2003, 2005; Sollins et al., 2009; Kaiser et al., 2015). For example, the clay size particles (< 2 μm), as those observed in casts (**Figures 5, 6**), are known to have high surface areas and adsorption capacities (Kögel-Knabner et al., 2008). In addition to mineral properties, living microorganisms produce polysaccharides during OM decomposition processes that favor adsorption of minerals and increase inter-particle cohesion (Chenu et al., 2002), leading to a strengthening of organo-mineral bonds in casts (Shipitalo and Protz, 1989).

In a unique way, the association of quantitative biogeochemical information and fine scale elemental and isotopic information led to depict the fate of shoot and root litter in earthworm casts. The chemical composition appeared as a driving parameter for litter degradation at the early stage



of decomposition in earthworm casts. A clear difference in the short-term (8 weeks) fate of shoot- and root- derived OC could be evidenced with a higher abundance of less degraded root residues recovered as particulate organic matter in the casts. After 1 year, the structural and chemical differences between shoots and roots ceased and the system dominated by plant-derived OM shifted toward a system where mineral-associated OM prevailed. Along with this shift, we demonstrate the buildup of microbial-dominated OM, both as living microbial biomass and dead microbial residues. Thus, microorganisms played a key role in litter degradation, producing binding agents for microaggregate formation and as an important carbon source in casts. These main findings are summarized in **Figure 7**. We emphasized the complex and dynamic role of earthworm casts as hot spots for OC inputs and microbial activity at the short term and potential stable carbon source at the longer term in soils. We were able to demonstrate the role of earthworms for the formation of presumably stable organo-mineral associations sequestering litter-derived carbon on longer timescales.

AUTHOR CONTRIBUTIONS

AV collected and analyzed the data, wrote the manuscript, and ensured the exchange between all co-authors. FW performed TEM analyses and gave technical and scientific support. LR performed nanoSIMS analyses and, gave technical and scientific support. CM supervised the sample fractionation and ^{13}C -NMR analyses and, gave technical and scientific support. T-TN participated in discussing the results obtained for the NanoSIMS and TEM analyses. FB realized the EA-IRMS analyses of the fractionated samples. SD and KQ participated to design the

experiment and supervised the project. All authors discussed the results and commented on the manuscript.

FUNDING

This study benefits from the financial support from the EC2CO program from the French National Institute of Sciences of the Universe (CNRS/INSU). The National NanoSIMS facility at the MNHN was funded by the CNRS, Région Ile de France, Ministère délégué à l'Enseignement supérieur et à la Recherche, and the MNHN. Part of this research was funded by the scientific program Action Thématiques du Muséum (Project WORMS). This work was supported by the German Research Foundation (DFG) and the Technical University of Munich (TUM) in the framework of the Open Access Publishing Program.

ACKNOWLEDGMENTS

Adriana Gonzalez-Cano (IMPMC) is acknowledged for the assistance on the NanoSIMS analyses, as well as Justine Paoli (Faculté de médecine—Université de Lorraine) for sample preparation. We also acknowledge Maria Greiner for the fractionation of cast samples. Part of the results of this work were presented in the doctoral thesis of AV.

SUPPLEMENTARY MATERIAL

The Supplementary Material for this article can be found online at: <https://www.frontiersin.org/articles/10.3389/fenvs.2019.00055/full#supplementary-material>

REFERENCES

- Angst, G., Heinrich, L., Kögel-Knabner, I., and Mueller, C. W. (2016). The fate of cutin and suberin of decaying leaves, needles and roots—inferences from the initial decomposition of bound fatty acids. *Organic Geochem.* 95, 81–92. doi: 10.1016/j.orggeochem.2016.02.006
- Angst, G., Mueller, K. E., Kögel-Knabner, I., Freeman, K. H., and Mueller, C. W. (2017). Aggregation controls the stability of lignin and lipids in clay-sized particulate and mineral associated organic matter. *Biogeochemistry* 132, 307–324. doi: 10.1007/s10533-017-0304-2
- Angst, Š., Mueller, C. W., Cajthaml, T., Angst, G., Lhotáková, Z., Bartuška, M., et al. Frouz, J. (2017). Stabilization of soil organic matter by earthworms is connected with physical protection rather than with chemical changes of organic matter. *Geoderma* 289, 29–35. doi: 10.1016/j.geoderma.2016.11.017
- Athmann, M., Kautz, T., Banfield, C., Bauke, S., Hoang, D. T. T., Lüsebrink, M., et al. (2017). Six months of *L. terrestris* L. activity in root-formed biopores increases nutrient availability, microbial biomass and enzyme activity. *Appl. Soil Ecol.* 120, 135–142. doi: 10.1016/j.apsoil.2017.08.015
- Baldock, J., Oades, J., Nelson, P., Skene, T., Golchin, A., and Clarke, P. (1997). Assessing the extent of decomposition of natural organic materials using solid-state ¹³C NMR spectroscopy. *Soil Res.* 35, 1061–1084. doi: 10.1071/S97004
- Baldock, J., and Skjemstad, J. (2000). Role of the soil matrix and minerals in protecting natural organic materials against biological attack. *Organic Geochem.* 31, 697–710. doi: 10.1016/S0146-6380(00)00049-8
- Balesdent, J., and Balabane, M. (1996). Major contribution of roots to soil carbon storage inferred from maize cultivated soils. *Soil Biol. Biochem.* 28, 1261–1263. doi: 10.1016/0038-0717(96)00112-5
- Barois, I., Villemin, G., Lavelle, P., and Toutain, F. (1993). Transformation of the soil structure through *Pontosclex corethrurus* (Oligochaeta) intestinal tract. *Geoderma* 56, 57–66. doi: 10.1016/0016-7061(93)90100-Y
- Baveye, P. C., Otten, W., Kravchenko, A., Balseiro-Romero, M., Beckers, É., Chalhoub, M., et al. (2018). Emergent properties of microbial activity in heterogeneous soil microenvironments: different research approaches are slowly converging, yet major challenges remain. *Front. Microbiol.* 9:01929. doi: 10.3389/fmicb.2018.01929
- Bi, Y.-M., Tian, G.-L., Wang, C., Feng, C.-L., Zhang, Y., Zhang, L.-S., et al. (2016). Application of leaves to induce earthworms to reduce phenolic compounds released by decomposing plants. *Eur. J. Soil Biol.* 75, 31–37. doi: 10.1016/j.ejsobi.2016.04.007
- Bonomi, G., Incerti, G., Giannino, F., Mingo, A., Lanzotti, V., and Mazzoleni, S. (2013). Litter quality assessed by solid state ¹³C NMR spectroscopy predicts decay rate better than C/N and Lignin/N ratios. *Soil Biol. Biochem.* 56, 40–48. doi: 10.1016/j.soilbio.2012.03.003
- Bossuyt, H., Denef, K., Six, J., Frey, S., Merckx, R., and Paustian, K. (2001). Influence of microbial populations and residue quality on aggregate stability. *Appl. Soil Ecol.* 16, 195–208. doi: 10.1016/S0929-1393(00)00116-5
- Bossuyt, H., Six, J., and Hendrix, P. F. (2005). Protection of soil carbon by microaggregates within earthworm casts. *Soil Biol. Biochem.* 37, 251–258. doi: 10.1016/j.soilbio.2004.07.035
- Brown, G. G. (1995). How do earthworms affect microfloral and faunal community diversity? *Plant Soil* 170, 209–231. doi: 10.1007/BF02183068
- Brown, G. G., Barois, I., and Lavelle, P. (2000). Regulation of soil organic matter dynamics and microbial activity in the drilosphere and the role of interactions with other edaphic functional domains. *Eur. J. Soil Biol.* 36, 177–198. doi: 10.1016/S1164-5563(00)01062-1
- Cameron, E. K., Cahill, J. F. Jr., and Bayne, E. M. (2014). Root foraging influences plant growth responses to earthworm foraging. *PLoS ONE* 9:e108873. doi: 10.1371/journal.pone.0108873
- Cepáková, Š., and Frouz, J. (2015). Changes in chemical composition of litter during decomposition: a review of published ¹³C NMR spectra. *J. Soil Sci. Plant Nutr.* 15, 805–815. doi: 10.4067/S0718-95162015005000055
- Chenu, C., and Plante, A. (2006). Clay-sized organo-mineral complexes in a cultivation chronosequence: revisiting the concept of the 'primary organo-mineral complex'. *Eur. J. Soil Sci.* 57, 596–607. doi: 10.1111/j.1365-2389.2006.00834.x
- Chenu, C., Stotzky, G., Huang, P., Bollag, J., and Senesi, N. (2002). *Interactions Between Microorganisms and Soil Particles: An Overview. Interactions Between Soil Particles and Microorganisms: Impact on the Terrestrial Ecosystem.* IUPAC. Manchester: John Wiley & Sons, Ltd., 1–40.
- Cortez, J., and Bouché, M. (1998). Field decomposition of leaf litters: earthworm-microorganism interactions—the ploughing-in effect. *Soil Biol. Biochem.* 30, 795–804. doi: 10.1016/S0038-0717(97)00164-8
- Cotrufo, M. F., Soong, J. L., Horton, A. J., Campbell, E. E., Haddix, M. L., Wall, D. H., et al. (2015). Formation of soil organic matter via biochemical and physical pathways of litter mass loss. *Nat. Geosci.* 8, 776–779. doi: 10.1038/ngeo2520
- Curry, J. P., and Schmidt, O. (2007). The feeding ecology of earthworms—a review. *Pedobiologia* 50, 463–477. doi: 10.1016/j.pedobi.2006.09.001
- Decaens, T. (2010). Macroecological patterns in soil communities. *Global Ecol. Biogeogr.* 19, 287–302. doi: 10.1111/j.1466-8238.2009.00517.x
- Dignac, M.-F., Bahri, H., Rumpel, C., Rasse, D., Bardoux, G., Balesdent, J., et al. (2005). Carbon-13 natural abundance as a tool to study the dynamics of lignin monomers in soil: an appraisal at the Coseaux experimental field (France). *Geoderma* 128, 3–17. doi: 10.1016/j.geoderma.2004.12.022
- Dignac, M.-F., Derrien, D., Barré, P., Barot, S., Cécillon, L., Chenu, C., et al. (2017). Increasing soil carbon storage: mechanisms, effects of agricultural practices and proxies. A review. *Agron. Sustain. Dev.* 37:14. doi: 10.1007/s13593-017-0421-2
- Drake, H. L., and Horn, M. A. (2007). As the worm turns: the earthworm gut as a transient habitat for soil microbial biomes. *Annu. Rev. Microbiol.* 61, 169–189. doi: 10.1146/annurev.micro.61.080706.093139
- Edwards, C. A. (2004). The importance of earthworms as key representatives of the soil fauna. *Earthworm Ecol.* 2, 3–11. doi: 10.1201/9781420039719.pt1
- Ekschmitt, K., Liu, M., Vetter, S., Fox, O., and Wolters, V. (2005). Strategies used by soil biota to overcome soil organic matter stability—why is dead organic matter left over in the soil? *Geoderma* 128, 167–176. doi: 10.1016/j.geoderma.2004.12.024
- Eusterhues, K., Rumpel, C., Kleber, M., and Kögel-Knabner, I. (2003). Stabilisation of soil organic matter by interactions with minerals as revealed by mineral dissolution and oxidative degradation. *Organic Geochem.* 34, 1591–1600. doi: 10.1016/j.orggeochem.2003.08.007
- Eusterhues, K., Rumpel, C., and Kögel-Knabner, I. (2005). Organo-mineral associations in sandy acid forest soils: importance of specific surface area, iron oxides and micropores. *Eur. J. Soil Sci.* 56, 753–763. doi: 10.1111/j.1365-2389.2005.00710.x
- Fahey, T. J., Yavitt, J. B., Sherman, R. E., Groffman, P. M., Fisk, M. C., and Maerz, J. C. (2011). Transport of carbon and nitrogen between litter and soil organic matter in a northern hardwood forest. *Ecosystems* 14, 326–340. doi: 10.1007/s10021-011-9414-1
- Filley, T., Cody, G., Goodell, B., Jellison, J., Noser, C., and Ostrofsky, A. (2002). Lignin demethylation and polysaccharide decomposition in spruce sapwood degraded by brown rot fungi. *Organic Geochem.* 33, 111–124. doi: 10.1016/S0146-6380(01)00144-9
- Frouz, J., Křišťufek, V., Livečková, M., Van Loo, D., Jacobs, P., and Van Hoorebeke, L. (2011). Microbial properties of soil aggregates created by earthworms and other factors: spherical and prismatic soil aggregates from unreclaimed post-mining sites. *Folia Microbiol.* 56, 36–43. doi: 10.1007/s12223-011-0011-7
- Frouz, J., Pižl, V., Cíenciala, E., and Kalčík, J. (2009). Carbon storage in post-mining forest soil, the role of tree biomass and soil bioturbation. *Biogeochemistry* 94, 111–121. doi: 10.1007/s10533-009-9313-0
- Hastings, A., Byers, J. E., Crooks, J. A., Cuddington, K., Jones, C. G., Lambrinos, J. G., et al. (2007). Ecosystem engineering in space and time. *Ecol. Lett.* 10, 153–164. doi: 10.1111/j.1461-0248.2006.00997.x
- Jouanin, L., and Lapierre, C. (2012). *Lignins: Biosynthesis, Biodegradation and Bioengineering.* Versailles Cedex: Academic Press.
- Kaiser, C., Kilburn, M. R., Clode, P. L., Fuchslueger, L., Koranda, M., Cliff, J. B., et al. (2015). Exploring the transfer of recent plant photosynthates to soil microbes: mycorrhizal pathway vs. direct root exudation. *N. Phytol.* 1537–1551. doi: 10.1111/nph.13138
- Kögel-Knabner, I., Guggenberger, G., Kleber, M., Kandeler, E., Kalbitz, K., Scheu, S., et al. (2008). Organo-mineral associations in temperate soils: integrating biology, mineralogy, and organic matter chemistry. *J. Plant Nutr. Soil Sci.* 171, 61–82. doi: 10.1002/jpln.200700048
- Kögel-Knabner, I., Hatcher, P. G., Tegelaar, E. W., and de Leeuw, J. W. (1992). Aliphatic components of forest soil organic matter as determined by solid-state ¹³C NMR and analytical pyrolysis. *Sci. Total Environ.* 113, 89–106. doi: 10.1016/0048-9697(92)90018-N
- Kuzyakov, Y., and Blagodatskaya, E. (2015). Microbial hotspots and hot moments in soil: concept & review. *Soil Biol. Biochem.* 83, 184–199. doi: 10.1016/j.soilbio.2015.01.025

- Lavelle, P. (2002). Functional domains in soils. *Ecol. Res.* 17, 441–450. doi: 10.1046/j.1440-1703.2002.00509.x
- Lavelle, P., Blanchart, E., Martin, A., Martin, S., and Spain, A. (1993). A hierarchical model for decomposition in terrestrial ecosystems: application to soils of the humid tropics. *Biotropica* 130–150. doi: 10.2307/2389178
- Lee, K. E. (1985). *Earthworms: Their Ecology and Relationships with Soils and Land Use*. Orlando, FL: Academic Press Inc.
- Lorenz, K., Lal, R., Preston, C. M., and Nierop, K. G. J. (2007). Strengthening the soil organic carbon pool by increasing contributions from recalcitrant aliphatic bio(macro)molecules. *Geoderma* 142, 1–10. doi: 10.1016/j.geoderma.2007.07.013
- Lu, Y., Watanabe, A., and Kimura, M. (2003). Carbon dynamics of rhizodeposits, root- and shoot-residues in a rice soil. *Soil Biol. Biochem.* 35, 1223–1230. doi: 10.1016/S0038-0717(03)00184-6
- Lubbers, I. M., Van Groenigen, K. J., Fonte, S. J., Six, J., Brussaard, L., and Van Groenigen, J. W. (2013). Greenhouse-gas emissions from soils increased by earthworms. *Nat. Climate Change* 3:187. doi: 10.1038/nclimate1692
- Lützw, M., Kögel-Knabner, I., Ekschmitt, K., Matzner, E., Guggenberger, G., Marschner, B., et al. (2006). Stabilization of organic matter in temperate soils: mechanisms and their relevance under different soil conditions—a review. *Eur. J. Soil Sci.* 57, 426–445. doi: 10.1111/j.1365-2389.2006.00809.x
- Martin, A. (1991). Short- and long-term effects of the endogeic earthworm *Millsonia anomala* (Omodeo)(Megascolecidae, Oligochaeta) of tropical savannas, on soil organic matter. *Biol. Fertility Soils* 11, 234–238. doi: 10.1007/BF00335774
- Miltner, A., Bombach, P., Schmidt-Brücken, B., and Kästner, M. (2012). SOM genesis: microbial biomass as a significant source. *Biogeochemistry* 111, 41–55. doi: 10.1007/s10533-011-9658-z
- Mueller, C. W., Brüggemann, N., Pritsch, K., Stoelken, G., Gayler, S., Winkler, J. B., et al. (2009). Initial differentiation of vertical soil organic matter distribution and composition under juvenile beech (*Fagus sylvatica* L.) trees. *Plant Soil* 323, 111–123. doi: 10.1007/s11104-009-9932-1
- Mueller, C. W., Gutsch, M., Kothieringer, K., Leifeld, J., Rethemeyer, J., Brüggemann, N., et al. (2014). Bioavailability and isotopic composition of CO₂ released from incubated soil organic matter fractions. *Soil Biol. Biochem.* 69, 168–178. doi: 10.1016/j.soilbio.2013.11.006
- Mueller, C. W., Weber, P. K., Kilburn, M. R., Hoeschen, C., Kleber, M., and Pett-Ridge, J. (2013). “Advances in the analysis of biogeochemical interfaces: NanoSIMS to investigate soil microenvironments,” in *Advances in Agronomy*, ed D. L. Sparks (Delaware, PA: Academic Press), 121, 1–46.
- Neuhaus, E. F., Hart-Nstein, R., and Connors, W. J. (1978). Soil invertebrates and the degradation of vanillin, cinnamic acid, and lignins. *Soil Biol. Biochem.* 10, 431–435. doi: 10.1016/0038-0717(78)90070-6
- Oades, J. (1988). The retention of organic matter in soils. *Biogeochemistry* 5, 35–70. doi: 10.1007/BF02180317
- Parle, J. (1963). A microbiological study of earthworm casts. *Microbiology* 31, 13–22.
- Pey, B., Cortet, J., Capowiez, Y., Nahmani, J., Watteau, F., and Schwartz, C. (2014). Technosol composition affects *Lumbricus terrestris* surface cast composition and production. *Ecol. Eng.* 67, 238–247. doi: 10.1016/j.ecoleng.2014.03.039
- Ponomareva, S. (1950). The role of earthworms in the creation of a stable structure in ley rotations. *Pochvovedenie* 1, 476–486.
- Preston, C. M., Nault, J. R., and Trofymow, J. (2009). Chemical changes during 6 years of decomposition of 11 litters in some Canadian forest sites. Part 2. ¹³C abundance, solid-state ¹³C NMR spectroscopy and the meaning of “lignin”. *Ecosystems* 12, 1078–1102. doi: 10.1007/s10021-009-9267-z
- Puget, P., and Drinkwater, L. E. (2001). Short-term dynamics of root- and shoot-derived carbon from a leguminous green manure. *Soil Sci. Soc. Am. J.* 65, 771–779. doi: 10.2136/sssaj2001.653771x
- Rasse, D. P., Rumpel, C., and Dignac, M.-F. (2005). Is soil carbon mostly root carbon? Mechanisms for a specific stabilisation. *Plant Soil* 269, 341–356. doi: 10.1007/s11104-004-0907-y
- Roman, I. A. M., Fischer, H., Mille-Lindblom, C., and Tranvik, L. J. (2006). Interactions of bacteria and fungi on decomposing litter: differential extracellular enzyme activities. *Ecology* 87, 2559–2569. doi: 10.1890/0012-9658(2006)87[2559:IOBAFO]2.0.CO;2
- Sánchez-de León, Y., Lugo-Pérez, J., Wise, D. H., Jastrow, J. D., and González-Meler, M. A. (2014). Aggregate formation and carbon sequestration by earthworms in soil from a temperate forest exposed to elevated atmospheric CO₂: A microcosm experiment. *Soil Biol. Biochem.* 68, 223–230. doi: 10.1016/j.soilbio.2013.09.023
- Shan, J., Liu, J., Wang, Y., Yan, X., Guo, H., Li, X., et al. (2013). Digestion and residue stabilization of bacterial and fungal cells, protein, peptidoglycan, and chitin by the geophagous earthworm *Metaphire guillelmi*. *Soil Biol. Biochem.* 64, 9–17. doi: 10.1016/j.soilbio.2013.03.009
- Shipitalo, M., and Protz, R. (1989). Chemistry and micromorphology of aggregation in earthworm casts. *Geoderma* 45, 357–374. doi: 10.1016/0016-7061(89)90016-5
- Six, J., Bossuyt, H., Degryze, S., and Denef, K. (2004). A history of research on the link between (micro) aggregates, soil biota, and soil organic matter dynamics. *Soil Tillage Res.* 79, 7–31. doi: 10.1016/j.still.2004.03.008
- Sollins, P., Kramer, M. G., Swanston, C., Lajtha, K., Filley, T., Aufdenkampe, A. K., et al. (2009). Sequential density fractionation across soils of contrasting mineralogy: evidence for both microbial- and mineral-controlled soil organic matter stabilization. *Biogeochemistry* 96, 209–231. doi: 10.1007/s10533-009-9359-z
- Tian, G., Brussaard, L., and Kang, B. (1995). Breakdown of plant residues with contrasting chemical compositions under humid tropical conditions: effects of earthworms and millipedes. *Soil Biol. Biochem.* 27, 277–280. doi: 10.1016/0038-0717(94)00182-Z
- Tuor, U., Winterhalter, K., and Fiechter, A. (1995). Enzymes of white-rot fungi involved in lignin degradation and ecological determinants for wood decay. *J. Biotechnol.* 41, 1–17. doi: 10.1016/0168-1656(95)00042-0
- van Veen, J. A., van Overbeek, L. S., and van Elsas, J. D. (1997). Fate and activity of microorganisms introduced into soil. *Microbiol. Mol. Biol. Rev.* 61, 121–135.
- Velasquez, E., Pelosi, C., Brunet, D., Grimaldi, M., Martins, M., Rendeiro, A. C., et al. (2007). This ped is my ped: visual separation and near infrared spectra allow determination of the origins of soil macroaggregates. *Pedobiologia* 51, 75–87. doi: 10.1016/j.pedobi.2007.01.002
- Vidal, A. (2016). *The fate of ¹³C Labelled Root and Shoot Litter in Soil and Earthworm Casts: A Multidisciplinary Approach Based on a Mesocosm Experiment*, Earth Sciences. Université Pierre et Marie Curie - Paris VI, Paris.
- Vidal, A., Quenea, K., Alexis, M., and Derenne, S. (2016a). Molecular fate of root and shoot litter on incorporation and decomposition in earthworm casts. *Organic Geochem.* 101, 1–10. doi: 10.1016/j.orggeochem.2016.08.003
- Vidal, A., Quenea, K., Alexis, M., Tu, T. N., Mathieu, J., Vaury, V., et al. (2017). Fate of ¹³C labelled root and shoot residues in soil and anecic earthworm casts: a mesocosm experiment. *Geoderma* 285, 9–18. doi: 10.1016/j.geoderma.2016.09.016
- Vidal, A., Remusat, L., Watteau, F., Derenne, S., and Quenea, K. (2016b). Incorporation of ¹³C labelled shoot residues in *Lumbricus terrestris* casts: a combination of transmission electron microscopy and nanoscale secondary ion mass spectrometry. *Soil Biol. Biochem.* 93, 8–16. doi: 10.1016/j.soilbio.2015.10.018
- Watteau, F., Villemain, G., Burtin, G., and Jocteur-Monrozier, L. (2006). Root impact on the stability and types of micro-aggregates in silty soil under maize. *Eur. J. Soil Sci.* 57, 247–257. doi: 10.1111/j.1365-2389.2005.00734.x
- Zangerlé, A., Pando, A., and Lavelle, P. (2011). Do earthworms and roots cooperate to build soil macroaggregates? A microcosm experiment. *Geoderma* 167, 303–309. doi: 10.1016/j.geoderma.2011.09.004
- Zelenev, V. V., van Bruggen, A. H., and Semenov, A. M. (2000). “BACWAVE,” a spatial-temporal model for traveling waves of bacterial populations in response to a moving carbon source in soil. *Microbial Ecol.* 40, 260–272. doi: 10.1007/s002480000029

Conflict of Interest Statement: The authors declare that the research was conducted in the absence of any commercial or financial relationships that could be construed as a potential conflict of interest.

Copyright © 2019 Vidal, Watteau, Remusat, Mueller, Nguyen Tu, Buegger, Derenne and Quenea. This is an open-access article distributed under the terms of the Creative Commons Attribution License (CC BY). The use, distribution or reproduction in other forums is permitted, provided the original author(s) and the copyright owner(s) are credited and that the original publication in this journal is cited, in accordance with accepted academic practice. No use, distribution or reproduction is permitted which does not comply with these terms.